Inorganic−Organic Hybrid Nonlinear Optical Films Containing Bulky Alkoxysilane Dyes

Lujian Chen, Guodong Qian,* Xuefeng Jin, Yuanjing Cui, Junkuo Gao, Zhiyu Wang, and Minquan Wang

Department of Materials Science and Engineering, State Key Lab of Silicon Materials, Zhejiang University, Hangzhou 310027, P. R. China

Received: November 13, 2006; In Final Form: January 30, 2007

Two bulky alkoxysilane dyes based on nonlinear optical (NLO)-active triphenylamino derivatives possessing high thermal stabilities, without and with a cyano group substitution on the vinylene moiety (TPAH and TPACN, respectively), were synthesized, characterized, and copolymerized with tetraalkoxysilane (TEOS) with the ratio of 1:5. After a poling and curing process, the resulting side-chain-type sol−gel films with excellent optical qualities were achieved. Second-order NLO coefficients, d_{33}, of 10−20 pm/V have been obtained in the films incorporated with different types of NLO-active dyes. The variation of chromophoric structures on NLO properties was investigated, indicating that the cyano substitution on the vinylene bridge of the chromophore would greatly enhance the temporal stability. This work provides a potential design strategy based on molecular engineering which would lead to more stable dipole orientation.

Introduction

Second-order nonlinear optics continues to be a topical area of research because of its tremendous potential in optoelectronic applications.[1] The fabrication of efficient photonic devices is a challenging task because such systems need to meet stringent requirements for high optical quality and for large and sustainable second-order nonlinear optical (NLO) response.[2] In the design of new photon-based materials for optical switching, data manipulation, and information processing, studies of both organic and inorganic materials have been pursued during the past decades.[3,4] Functionalized main-chain- and side-chain-type polymers with NLO-active chromophores have been extensively studied for future NLO applications because of their inexpensive, relatively easy-to-prepare, and good film-processing properties for waveguide device fabrication.[4,5] They can also be readily integrated with semiconductor electronics and fiber-optic transmission lines. As a result, polymeric materials promise to make optoelectronic technologies more practical and widespread.

The so-called sol−gel methodology for the processing of glassy materials allows low-temperature fabrication of crosslinkable networks facilitating the introduction of organic chromophores, and the resulting hybrids possess high T_g, show low beam propagation loss, and are more stable because of the greater rigidity and higher thermal stability of silica than organic polymers.[3,6] The optical response and its temporal stability are strongly dependent on the nature of bonding between the organic chromophores and the matrix.[7,8] The random orientation of NLO-active dyes in sol−gel matrixes rules out second-harmonic generation (SHG). Second-order nonlinearities can only be observed when the NLO-active dyes within the sol−gel matrix are effectively oriented after poling.

The incorporation of organic NLO-active molecules with enhanced hyperpolarizabilities into different bulk components has been the focus of recent research interests.[9−11] These interests are also motivated by the possibility of tailoring the physicochemical properties by the molecular engineering approach. Dalton's group and Jen's group have made pioneering works.[9,10] Their collaborators have incorporated the chromophores into various matrixes including sol−gels.[11] Traditionally, these NLO-active molecules with a long-conjugated bridge were always thermally unstable. As we know, the temporal stability of the poling-induced alignment of the chromophores is important for long-term device efficiency and is increased if high T_g sol−gel host materials are used.[12] So these chromophores must be sufficiently thermally robust at high temperatures to withstand the poling process and other fabrication steps for those devices. On the basis of the above considerations, triphenylamine derivatives attract our attentions.[13,14] Among various classes of NLO-active chromophores, bulky triphenylamine derivatives with a higher decomposition temperature are very promising candidates because of their multifunctional properties, such as two-photon absorption and hole-conducting properties.[15−17]

In this investigation, we reported inorganic/organic NLO materials based on two bulky triphenylamino-based alkoxysilane dyes (ICTES-TPAH and ICTES-TPACN; Scheme 1). Characterizations of the chromophores, named TPAH and TPACN, are presented in details by element analysis, FTIR, ^{1}H NMR, UV−vis spectra, thermogravimetric analysis (TGA), and differential scanning calorimetry (DSC). The first molecular hyperpolarizabilities of the corresponding chromophores were acquired by the solvatochromic method. The Maker Fringe method was used to measure the macroscopic nonlinearities of the sol−gel films.[18,19] And the thermal dynamic and temporal stability behaviors of the NLO sol−gel films were also studied by in-situ SHG measurement and compared. Previously, we reported the covalent incorporation of isophorone chromophores with different size into sol−gel systems, revealing that the bulkier triphenylamino-based one has a less stable orientation after the same poling procedure.[20] It was found here that the cyano substitution on the central phenylene ring of such a bulky D-π-A molecule would lead to a slower relaxation of the dipolar orientation over time.

* Corresponding author. Tel.: +86-571-87952334. Fax: +86-571-87951234. E-mail: gdqian@zju.edu.cn.

10.1021/jp0674975 CCC: $37.00 © 2007 American Chemical Society
Published on Web 03/07/2007

SCHEME 1: Chemical Diagram of Alkoxysilane Dyes in This Study

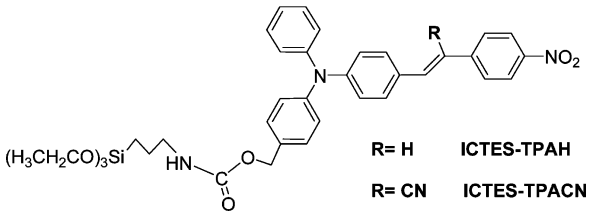

Experimental Section

Materials. All starting chemicals such as triphenylamine, 4-nitrophenylacetic acid, 4-nitrophenylacetonitrile, and 3-isocyanatopropyltriethoxysilane (ICTES) were obtained from ACROS, Alfa Aesar, and TCI. Phosphorus oxychloride ($POCl_3$) and sodium borohydride were purchased from Shanghai Tingxin Chemical & Reagent Co and Sinopharm Chemical reagent Co., Ltd., respectively. These materials were used as received. Tetrahydrofuran (THF) was dried over calcium hydride and distilled under vacuum. Other solvents, of analytical-grade quality, were commercial products and used as received.

Intermediates. The triphenylamine intermediates were synthesized via Vilsmeier-Haack formylation and selective reduction of one aldehyde group, and the details can be found in other references.[15,17]

4,4′-(Phenylazanediyl)dibenzaldehyde (1). Yield: 63%. ^{1}H NMR (500 MHz, $CDCl_3$, δ ppm): δ 7.17−7.19 (m, 6H, Ar**H**), δ 7.25−7.28 (t, 1H, Ar**H**), δ 7.38−7.41 (t, 2H, Ar**H**), δ 7.76−7.78 (d, 4H, Ar**H**), δ 9.89 (s 2H, C**H**O). Anal. Calcd for $C_{20}H_{15}NO_2$ (301.34): C, 79.72; H, 5.02; N, 4.65. Found: C, 79.65; H, 5.07; N, 4.75.

4-((4-(Hydroxymethyl)phenyl)(phenyl)amino)benzaldehyde (2). Yield: 72%. ^{1}H NMR (500 MHz, $CDCl_3$, δ ppm): δ 1.85 (s, 1H, −Ph−CH_2−O**H**), δ 4.69 (s, 2H, −Ph−C**H**$_2$−OH), δ 7.15−7.18 (t, 5H, Ar**H**), δ 7.32−7.35 (t, 4H, Ar**H**), δ 7.66−7.68 (d, 2H, Ar**H**), δ 9.80 (s, 1H, C**H**O).

Triphenylamine-Based Chromophores. To a solution of 2.5 g (8.3 mmol) of 4-((4-(hydroxymethyl)phenyl)(phenyl)amino) benzaldehyde (2) and 1.9 g (10 mmol) of 4-nitrophenylacetic acid in 20 mL of pyridine, a few drops of piperidine were added as catalyst. The reaction mixture was stirred at 120 °C for 5 h, cooled, poured onto ice, extracted with dichloromethane, and dried by $MgSO_4$. After filtration the solvent was evaporated, and the crude reaction product was purified first by column chromatography onto silica gel and dichloromethane as eluent. After evaporation of the solvent, the remaining reaction product was recrystallized from ethanol to obtain pure chromophore 3. The chromophore TPACN (4) could also be obtained by reacting 4-((4-(hydroxymethyl)phenyl)(phenyl)amino)
benzaldehyde (2) with 4-nitrophenylacetonitrile for 3 h under conditions similar to those for the preparation of TPAH (3).

(4-((4-(4-Nitrostyryl)phenyl)(phenyl)amino)phenyl)-methanol (TPAH, 3). Yield: 42%. mp: 146.4 °C. ^{1}H NMR (500 MHz, $CDCl_3$, δ ppm): δ 1.56 (s, 1H, −Ph−CH_2−O**H**), δ 4.69 (s, 2H, −Ph−C**H**$_2$−OH), δ 7.00−7.03 (d, 1H, CH═C**H**, J = 16.3), δ 7.05−7.13 (m, 8H, Ar**H**), δ 7.20−7.23 (d, 1H, C**H**═CH, J = 16.3), δ 7.27−7.30 (m, 3H, Ar**H**), δ 7.40−7.42 (d, 2H, Ar**H**), δ 7.59−7.60 (d, 2H, Ar**H**), δ 8.19−8.21 (d, 2H, Ar**H**). Anal. Calcd for $C_{27}H_{22}N_2O_3$ (422.48): C, 76.76; H, 5.25; N, 6.63. Found: C, 76.78; H, 5.24; N, 6.58.

3-(4-((4-(Hydroxymethyl)phenyl)(phenyl)amino)phenyl)-2-(4-nitrophenyl)acrylonitrile (TPACN, 4). Yield: 53%. mp: 73.8 °C. ^{1}H NMR (500 MHz, $CDCl_3$, δ ppm): δ 1.56 (s, 1H, −Ph−CH_2−O**H**), δ 4.70 (s, 2H, −Ph−C**H**$_2$−OH), δ 7.03−7.05 (d, 2H, Ar**H**), δ 7.17−7.18 (t, 5H, Ar**H**), δ 7.33−7.36 (m, 4H, Ar**H**), δ 7.55 (s, 1H, C**H**═C(CN)), δ 7.79−7.83 (m, 4H, Ar**H**), δ 8.27−8.29 (d, 2H, Ar**H**). Anal. Calcd for $C_{28}H_{21}N_3O_3$ (447.48): C, 75.15; H, 4.73; N, 9.39. Found: C, 74.82; H, 4.69; N, 9.14.

Alkoxysilane Dyes. *General Procedure*. A dry, 50-mL three-necked flask equipped with an oil bath, a mechanical stirrer, a nitrogen inlet, and a reflux condenser was charged with 4 mmol chromophore, 3-isocyanatopropyltriethoxysilane (ICTES, 1.19 g, 4.8 mmol), 15 mL of THF, and 5 drops of triethylamine (TEA) as catalyst. The reaction mixture was stirred and refluxed for 48 h under nitrogen atmosphere.[7] The resulting alkoxysilane dye was purified by flash column chromatography onto silica gel using petroleum ether/ethyl acetate (2:3, v/v) as eluent.

ICTES-TPAH. Yield: 35%. FTIR (KBr pellet, cm^{-1}): 3340 (−NH), 1716 (−C═O), 1585 (−C_6H_4), 1508 (−NO_2, ν_{as}), 1338 (−NO_2, ν_s), 1107, 1076 (Si−O−CH_2CH_3). ^{1}H NMR (500 MHz, DMSO-d_6, δ ppm): δ 0.52−0.55 (t, 2H, $CH_2CH_2CH_2$), δ 1.12−1.16 (m, 9H, CH_2CH_3), δ 1.45−1.48 (t, 2H, $CH_2CH_2CH_2$), δ 2.96−3.00 (m, 2H, $CH_2CH_2CH_2$), δ 3.71−3.75 (m, 6H, CH_2-CH_3), δ 4.97 (s, 2H, NArC**H**$_2$O), δ 6.95−6.97 (d, 2H), δ 7.03−7.12 (m, 5H), δ 7.24−7.36 (m, 6H), δ 7.46−7.49 (d, 1H), δ 7.56−7.58 (d, 2H), δ 7.81−7.83 (d, 2H), δ 8.20−8.22 (d, 2H).

ICTES-TPACN. Yield: 31%. FTIR (KBr pellet, cm^{-1}): 3340 (−NH), 2210 (−CN), 1716 (−C═O), 1573 (−C_6H_4), 1506 (−NO_2, ν_{as}), 1340 (−NO_2, ν_s), 1109, 1078 (Si−O−CH_2CH_3). ^{1}H NMR (500 MHz, DMSO-d_6, δ ppm): δ 0.51−0.55 (t, 2H, $CH_2CH_2CH_2$), δ 1.12−1.15 (m, 9H, CH_2CH_3), δ 1.45−1.48 (t, 2H, $CH_2CH_2CH_2$), δ 2.97−3.00 (m, 2H, $CH_2CH_2CH_2$), δ 3.71−3.75 (m, 6H, CH_2CH_3), δ 5.00 (s, 2H, NArC**H**$_2$O), δ 6.93−6.95 (d, 2H), δ 7.13−7.25 (m, 6H), δ 7.36−7.41 (m, 4H), δ 7.90−7.91 (d, 2H), δ 7.96−7.97 (d, 2H), δ 8.13 (s, 1H), δ 8.29−8.31 (d, 2H).

Sol−Gel Processing and Film Preparation. Each of the alkoxysilane dyes was mixed with TEOS with a molar ratio of 1:5 in THF to prepare the coating solution. Then acidic water (HCl, pH = 1) was added to favor the cohydrolysis/condensation process, the H_2O/Si molar ratio was 4:1. To increase the viscosity, the solution was stirred at room temperature for 3 h and aged for 7 days. The sol was filtered through a 0.22-μm Teflon membrane filter before spin coating on the glass substrates or the indium−tin−oxide (ITO) substrates. The coated films were vacuum-dried at 80 °C for 2 h to remove the residual solvent.

Characterization. Elemental analysis was carried out on an Eager 300 microelemental analyzer. ^{1}H NMR spectra were obtained with a Bruker Avance DMX500 spectrometer using tetramethysilane (TMS) as an internal standard. FTIR spectra were recorded on a Nicolet Avatar 360 in the region of 4000−400 cm^{-1} using KBr pellets. UV−vis absorption spectroscopic study was performed with a Perkin-Elmer Lambda 20 spectrophotometer. The decomposition temperature was studied using a TA Instruments SDT Q600 at a heating rate of 10 °C/min in nitrogen atmosphere. A TA Instruments SDT Q100, with a heating rate of 10 °C/min, was used to study the differential scanning calorimetry (DSC) in nitrogen atmosphere. The thickness and the index of thin films were determined using the Metricon PC 2010 prism coupler.

Second Harmonic Generation (SHG) Measurement. The second-order optical nonlinearity of hybrid films was determined by SHG measurement. The laser source is a Q-switched Nd:YAG pulse laser with a 1064-nm fundamental beam (500-mJ maximum energy, 3−5-ns pulse width, and 10-Hz repeating rate). A Y-cut quartz crystal (d_{11} = 0.5 pm/V) was used as

SCHEME 2: Synthesis of the NLO Alkoxysilane Dyes

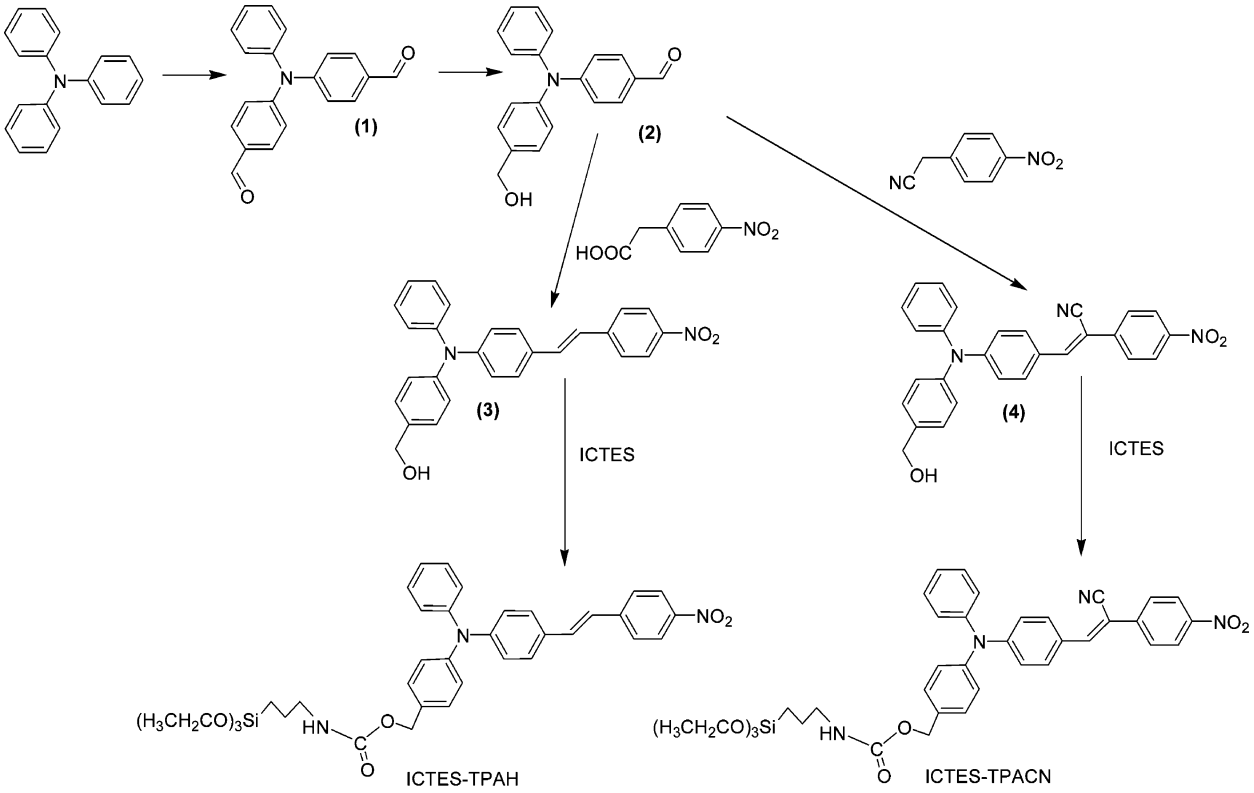

reference. For in-situ poling experiments, a closed temperature-controlled oven having optical windows and equipped with tungsten needle electrodes was used. The film deposited on the ITO substrate, which remained at 45° to the incident beam, was in-situ poled at 4.5 kV inside the oven to monitor the dependence of in-situ SHG intensity on poling temperature. The gap distance between the tungsten needle and the film is 1 cm. Temperature dependence of the dipole reorientation of the NLO polymers can be observed via the decay of effective SHG coefficients (d_{eff}) at various temperatures. Relaxation behaviors were investigated by monitoring the decay of the d_{eff} as a function of time at various temperatures.

Results and Discussion

Synthesis and Characterization. The overall synthesis route of the two alkoxysilane dyes is schematized in Scheme 2. Both of the NLO chromophores with a high thermal decomposition temperature of about 300 °C were synthesized via Knoevenagel condensation[21] and then further reacted with ICTES to give functional sol−gel precursors via a urethane-forming reaction. Followed by the hydrolysis and copolymerization process of alkoxysilane dyes, two kinds of inorganic−organic hybrid films covalently incorporated with different NLO chromophores were prepared. The addition of TEOS was intended to increase the cross-linking density of the silica matrix. The thickness of the films was at the range of 0.4−0.6 μm. As shown in Figure 1, the FTIR spectra confirmed the successful incorporation of chromophore into the silica network. In the FTIR spectra, both films showed two strong sharp peaks at about 1506 and 1340 cm^{-1}, attributable to the asymmetric and symmetric stretching vibration of the nitro group in the chromophores, as well as a large absorption band between 1200 and 1000 cm^{-1} due to the Si−O−Si stretching vibration. An additional absorption peak located at 2210 cm^{-1}, corresponding to the cyano group, was maintained in the film containing TPACN after the sol−gel process. The spin-coated hybrid films are tough and resistant to organic solvents. Good solvents for the alkoxysilane dyes, for example, THF, and so forth, could not extract any measurable concentration of the dyes from the vacuum-dried films, indicating that the chromophore were firmly covalently incorporated into the silica matrix.

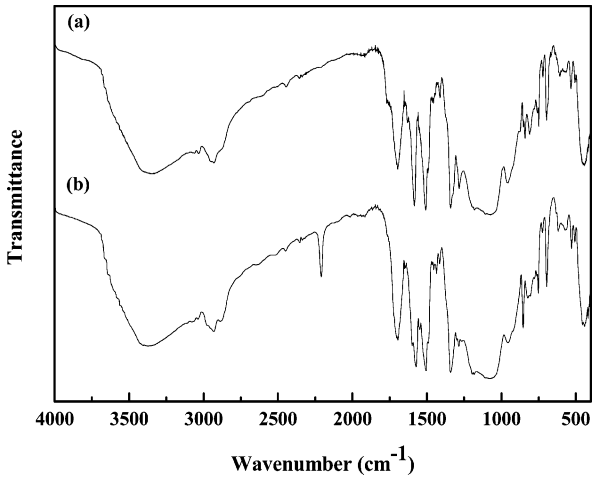

Figure 1. FTIR spectra of the xerogel with TPAH (a) and TPACN (b).

Thermal Properties of the Hybrid Materials. The thermal stability of the hybrid materials was studied by the TGA method, and the differentiated curves of the weight lost were also presented in Figure 2. Both of the hybrids represented a two-stage decomposition behavior at different temperature ranges. The first stage, from 200 to 400 °C, consisted of the breaking of the carbamate linkage between the NLO-active dye and the sila-functional alkoxy groups and the initial decomposition of NLO-active dye. And the second stage, above 400 °C, revealed the further carbonization of the residual organic component. However, DSC of the vacuum-dried sol−gel-derived hybrid

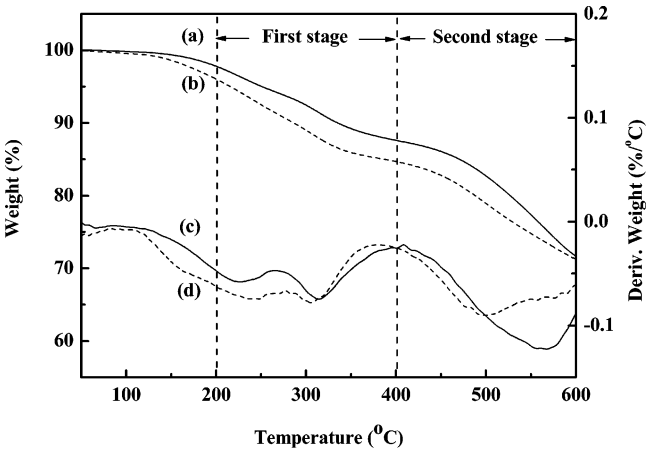

Figure 2. TGA curves of the xerogel with TPAH (a) and TPACN (b), and the differential weight loss curves of TPAH-based (c) and TPACN-based (d) xerogel.

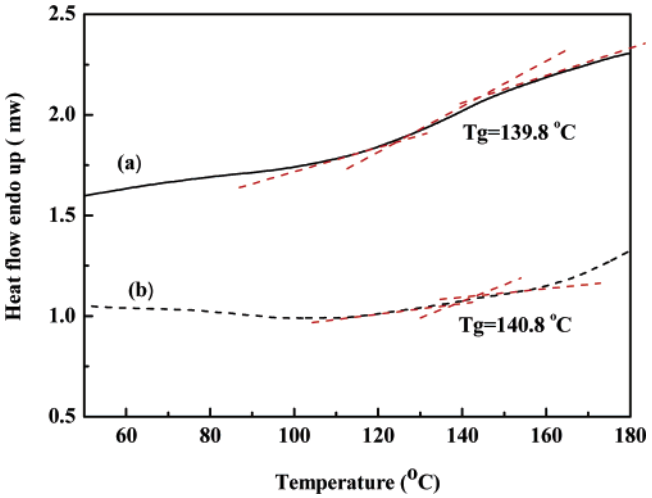

Figure 3. DSC curves of xerogel with TPAH (a) and TPACN (b).

TABLE 1: Characterization of Chromophores

chromophores	T_d[a] (°C)	λ_{max}[b] (nm)	$\mu_g\beta$[c] (10^{-30} esu D)
TPAH	298.4	424	891
TPACN	300.7	450	1096

[a] Decomposition temperature taken as the temperature corresponding to the onset in the TGA curves. [b] Measured in THF. [c] Acquired by the solvatochromic method.

materials were still in debate, and always failed to show clear glass transition behaviors unambiguously. The DSC curves of the hybrids containg TPAH and TPACN were also investigated in the temperature range 50−180 °C as depicted in Figure 3. Traditionally, these behaviors are indicative of the broad distribution of T_g due to a slow and incomplete cross-linking process in the thermal treatment of the films. But if the glass transition behaviors were assumed to exist in the hybrids investigated here, T_g of the hybrids with TPAH and TPACN could be determined to be 139.8 and 140.8 °C by the accessorial software of TA Instruments SDT Q100, respectively.

Linear Optical Properties. When an additional strong electron-withdrawing group (−CN) is designed to be introduced at the position of vinylene, the structure change of the acceptor can cause an increased electron-release behavior and change the resonance absorption. As shown in Table 1, the red-shift of the typical absorption maximum (λ_{max}), which is contributed by the $\pi-\pi^*$ electronic transition, can possibly occur. Both of the dipolar NLO chromophores showed a bathochromic shift due to the well-known solvatochromic effect when incorporated into silica sol−gel films, as listed in Table 2. This phenomenon was also reported previously and can be explained by the different environment around the NLO dyes provided by the sol−gel matrix. A red-shift of the absorption maximum indicating the recovery from dimer to monomer structure was usually observed in this type of materials after thermal treatment;[22] however, in our study, no shift and broadening of the absorption maximum of sol−gel films with TPAH and TPACN was found. In other words, the bulky chromophore with a diaryl group has a quinoidal bonding pattern, which may help to prevent unfavorable organization of the chromophores, making the antiparallel alignment of two neighboring molecules less efficient.[23]

The refractive index (RI) and thickness for the hybrid films are measured using the prism coupling method at wavelengths of 632.8 and 1300 nm. The wavelength dispersion of RI, $n(\lambda)$, can be fitted to a one-oscillator Sellmeier-dispersion formula:[24]

$$n^2(\lambda) - 1 = \frac{q}{1/\lambda_0^2 - 1/\lambda^2} + A \qquad (1)$$

where λ_0 is the absorption wavelength of the dominant oscillator, q is a measure for the oscillator strength, and A is a constant containing the sum of all the other oscillators. Thickness and RI values at 532 and 1064 nm obtained from the plot are also listed in Table 2.

Nonlinear Optical Properties. The first hyperpolarizability of the chromophores was simply approached by determination of the UV−vis absorption spectra in different solvents using a two-level model. Using solvatochromic methods,[25,26] the microscopic nonlinearity, $\mu\beta$ value of the chromophore TPACN was calculated to be 23% higher than that of TPAH with a wavelength of 1064 nm. The result evidenced once more that the substituent CN group at the position of vinylene could bring considerable improvement in β-value due to the increase of the accepter strength. The NLO prosperity of the resulting poled sol−gel film was also examined by measuring SHG in transmission from the thin film on the ITO glass substrate. A typical Maker Fringe pattern of the poled film (TPAH) is shown in Figure 4. The second harmonic coefficient (d_{33}) of the hybrid films can be calculated by comparison with the SHG intensity of a standard Y-cut quartz crystal plate.[18,19] From the calculation, we obtained the d_{33} values of the films containing TPAH and TPACN, after poling at 140 °C for 1 h, as listed in Table 2.

In our study, the poling voltage was set at a constant 4.5 kV for different films with different thicknesses on ITO glasses, and the poling current was not monitored synchronously. It is well-known that, under the same static electric field, the thicker

TABLE 2: Linear and Nonlinear Optical Properties of Hybrid Films

			refractive index				
hybrid films	thickness (μm)	λ_{max} (nm)	532 nm	632.8 nm	1300 nm	1064 nm	d_{33} (pm/V)
film-TPAH	0.417	434	1.702	1.655	1.624	1.620	16.7
film-TPACN	0.550	459	1.733	1.642	1.582	1.576	14.1

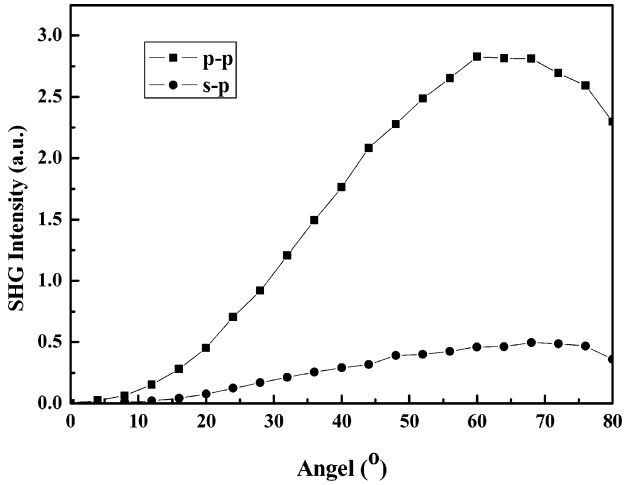

Figure 4. Maker Fringe patterns for the poled sol−gel film with TPAH.

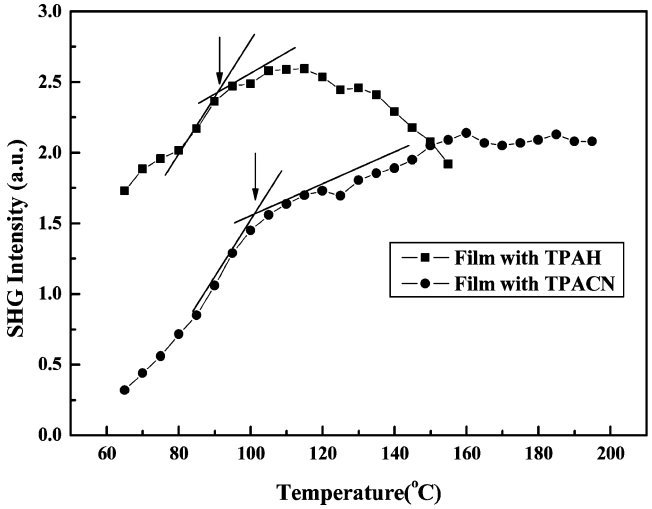

Figure 5. Dependence of in-situ SHG intensity on poling temperature.

film will stand a smaller electric current. The TPAH-based thin film (with a thickness of 417 nm) could be oriented more effectively than the TPACN-based thicker film (530 nm), and results in an inconsistency of the microscopic and macroscopic NLO coefficient. The stronger interaction between the TPACN molecule and the sol−gel matrix might also hinder the dipole to be effectively oriented after corona poling. The moderate d_{33} values could be ascribed to the weak orientation mobility of the bulky molecules.

Temperature-Dependence Study of In-Situ Poling Process. Traditionally, the in-situ poling technique was used to optimize the poling temperature in order to get the largest second-order NLO response. As shown in Figure 5, the temperature dependence of the NLO response of the films was observed. With the rising of temperature, more and more chromophores in the film were oriented along the electric field due to the greater mobility of the matrix. The SHG signal of the TPAH film rose with increasing poling temperature; after a maximum at 110 °C was reached, the SHG signal began to drop. But for TPACN film, the SHG signal reached a maximum at 160 °C, and no significant drop was found until 195 °C.

For a pure polymer matrix, it was clear that the maximum of the SHG intensity was defined as "the optimum poling temperature" and was closely related to the glass transition temperature (T_g) of the films.[27] However, the coated sol−gel films are composed of partly condensed organosilicates. This is why the chromophores in the cross-linking type organosilicate

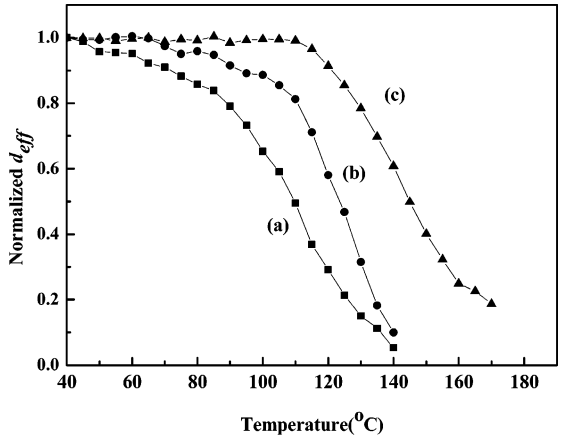

Figure 6. Decay of the normalized d_{eff} values as a function of temperature for the film with TPAH poled at 140 °C for 1 h (a), the film with TPACN poled at 140 °C for 1 h (b), and the film with TPACN poled at 200 °C for 1 h (c).

films are still able to be aligned under the electric field. The following explanation can account for this observed effect. In hybrid films, with the rising of temperature, chromophores will acquire more and more mobility and the dipole is easier to align along the electric field. If the interaction between the NLO dye and the matrix was stronger, a maximum of the SHG intensity would appear at higher temperature. It can be concluded that TPACN has a stronger interaction with the sol−gel matrix than TPAH.

The polycondensation reaction rate in the sol−gel film system is extremely slow at room temperature, but it is always faster when the temperature is elevated. So it is difficult to determine the extract relationship between T_g and the "the optimum poling temperature" in sol−gel materials. Besides, a higher poling temperature converts the wet gel into the dry gel with a more condensed structure, further confining the chromophore's rotational movement. It is therefore desired to raise the poling temperature as high as possible.[28] The formation of smaller free volumes in rigid inorganic networks would potentially help freeze the chromophore molecules. But in this study, our main purpose was to examine the influence of CN substitution on the thermal dynamic stability, so a moderate poling temperature (corresponding to T_g = 140 °C) was adequate for a valid comparison.

Thermal Dynamic and Temporal Relaxation Behaviors. Thermal dynamic stability of the poled films was investigated by depoling experiments, that included heating the poled sample in the absence of a poling electric field and measuring the decrease of SHG signal at a rising rate of 10 °C/min from 40 to 150 °C, as shown in Figure 6. The half-decay temperature, at which the d_{eff} value corresponded to half of the initial value, was about 110 °C and 125 °C for TPAH- and TPACN-based films poled at 140 °C for 1 h, respectively. Apparently, two stages of dipolar reorientation existed in the film with TPACN. At the lower operating temperature, a stable SH signal was maintained. When the operating temperature was beyond 80 °C, an evident decay of the SH signal was observed. In contrast, the dipolar alignment in TPAH film seems to be more susceptible to the heating process. It is desired to raise the poling temperature as high as possible. The film containing the thermally stable TPACN molecule was poled at 200 °C for 1 h to evaluate the best orientation stability that we could achieve in this sol−gel system. It was found that the SH signal was stable until 115 °C and the half-decay temperature was about 145 °C.

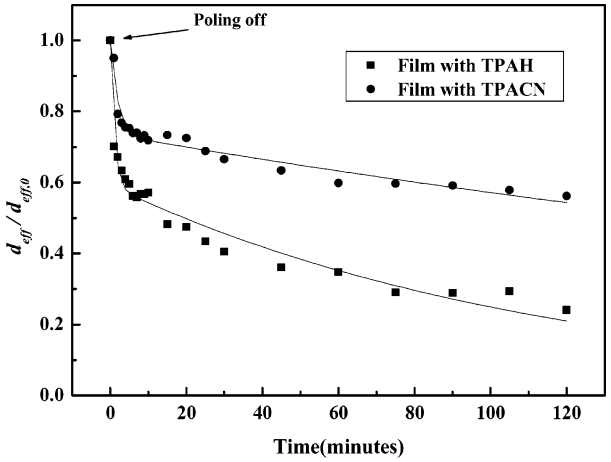

Figure 7. Temporal stability of the normalized d_{eff} values of the films poled at 140 °C for 1 h after the electric field was removed at 100 °C.

TABLE 3: Parameters for the Relaxation of the Normalized d_{eff} at 100 °C

hybrid films	A	τ_1 (min)	τ_2 (min)
film-TPAH	0.40798	1.06184	115.57862
film-TPACN	0.26374	1.94072	394.96158

To further understand the thermal behavior of the hybrid film, temporal relaxation behaviors for the hybrid films were also studied. Both of the films were poled at 140 °C for 1 h. After the temperature reached 100 °C, we turned off the voltage to observe the decay of the SH signal. Figure 7 shows the time-dependent decay of the effective second harmonic coefficient (d_{eff} value) of the poled films. The d_{eff} fell to 72% of the initial value within 10 min for TPAH and about 57% for TPACN. The decay curves of the d_{eff} value can be fitted to a biexponential function:[29]

$$\frac{d_{eff}(t)}{d_{eff}(0)} = A\cdot\exp\left(-\frac{t}{\tau_1}\right) + (1-A)\cdot\exp\left(-\frac{t}{\tau_2}\right) \qquad (2)$$

where A is the amplitude of the rapid decay regime, and τ_1 and τ_2 are the time constants that characterize the rapid and slow decay of chromophore orientation in the matrix, respectively. The A value and relaxation times τ_1 and τ_2 were calculated and are presented in Table 3. It was found that the TPACN-based NLO film had a decreased parameter A and increased τ_1 and τ_2 values relative to those of the TPAH-based film.

It was reported before that the condensation of polyfunctional alkoxysilanes is always difficult to complete.[7,30] The weak cross-linking efficiency can be due to the dye size. In our previous study, a bulky diphenyl group located at the donor side of the NLO dyes was found to influence the hydrolysis and copolymerization process of the dye-bonded precursor with TEOS and led to less stable nonlinearities over time than its diaryl analogue.[20] This phenomenon may prevent many promising bulky NLO alkoxysilane dyes such as triphenylamine derivatives from some NLO applications when temporal stability is of paramount importance.

The FTIR spectra show a broad and overlapped band around 3403 cm^{-1} in both of the films, which were similarly assigned to hydrogen-bonded and isolated NH stretching vibration modes. As indicated in the article, the absorption band at 1698 cm^{-1} can be ascribed to the hydrogen-bonded carbonyl stretching vibrations in carbamate. The SHG signal started to increase rapidly around 80−100 °C (Figure 5). This temperature coincided roughly with the temperature at which hydrogen bonds start to be disorganized. And the decay of the NLO effect in the first stage (Figure 6) could also partially be ascribed to the collapse of the hydrogen bond between side groups. However, for the film poled efficiently at elevated temperature, the further condensation of Si−OH groups would lead to a stable dipolar orientation. It should be addressed that the hydrogen bond or other interactions between molecules and the matrix would play an important role in the NLO behaviors.

In the comparative study presented here, it was surprising and encouraging to find out that the introduction of cyano substitution on the vinylene of the bulky stilbene dye would enhance its dipolar reorientation stability in the sol−gel matrix. Assuming that both of the bulky alkoxysilane precursors would possess similar hydrolysis and copolymerization processes and lead to films with resembling structures, which could also be confirmed by the thermal analysis as described previously, a proper explanation of the situation should take the difference after the incorporation of the cyano group into consideration.

We speculate that there are two probable explanations for the phenomena. First, the remaining Si−OH due to the incomplete condensation may form an additional hydrogen bond with the cyano group and/or the COOH group derived from the partial hydroxylation of the cyano group under acid condition. Second, a superior long-term stability of dialkoxyl analogues after cyano substitution was found in a well-known PMMA matrix lack of ability to form a hydrogen bond.[27] The strong distortion of the π-backbone has always been observed for the cyano-substituted distyrylbenzenes in solid states revealed by the single-crystal X-ray diffraction method and quantum chemical calculation.[31−34] The cyano group lies in approximately the same plane as the vinylene linkage but not in the plane of any of the rings. And the steric hindrance between the cyano groups and the hydrogens on the phenylene ring on the triphenylamino donor (P_D) and the phenylene rings on the electro acceptor (P_A) would properly lead to a strong distortion of the π-backbone. A larger angle (over 70°) between the planes defined by P_D and P_A in the TPACN molecule than in TPAH, and an additional steric interaction caused by the cyano group in TPACN could be expected. The entanglement of the resulting twisted "hook-like" chromophore with the C−C chain in PMMA or Si−O−Si structure in sol−gel materials might provide a stronger interaction in the film. The two possibilities (or one of them) determine that TPACN is more difficult to rotate than TPAH in the same matrix and under the same condition.

Conclusion

In this study, two new inorganic−organic hybrid films covalently incorporated with diarylamino-substituted stilbene chromophores without and with the cyano substitution were prepared by the sol−gel technique. SHG measurement indicated that the second harmonic coefficients (d_{33}) at 1064 nm of hybrid films were 10−20 pm/V. The additional interaction provided by the cyano substitution on the vinylene moiety of the chromophore and the matrix may play an important role on the enhanced temporal stability of the oriented dipole, which provides a potential design strategy based on molecular engineering.

Acknowledgment. The authors gratefully acknowledge the financial support for this work from the National Natural Science Foundation of China (under Grant Nos. 50532030 and 50625206), the China Postdoctoral Science Foundation (No. 20060400310) and the Postdoctoral Research Project of Zhejiang Province (No. 2006-bsh-01).

References and Notes

(1) Prasad, P. N.; Williams, D. J. *Introduction to Nonlinear Optical Effects in Molecules and Polymers*; John Wiley & Sons, Inc.: New York, 1991. Zyss, J. *Molecular Nonlinear Optics Materials Physics and Devices*; Academic Press: Orlando, 1994.

(2) Marder, S. R.; Perry, J. W. *Science* **1994**, *263*, 1706. Marder, S. R.; Kippelen, B.; Jen, A. K.-Y.; Peyghambarian, N. *Nature* **1997**, *388*, 845. Shi, Y.; Zhang, C.; Zhang, H.; Bechtel, J. H.; Dalton, L. R.; Robinson, B. H.; Steier, W. H. *Science* **2000**, *288*, 119.

(3) Chaumel, F; Jiang, H. W.; Kakkar, A. *Chem. Mater.* **2001**, *13*, 3389. Lacroix, P. G. *Chem. Mater.* **2001**, *13*, 3495. Innocenzia, P.; Lebeau, B. *J. Mater. Chem.* **2005**, *15*, 3821.

(4) Samyn, C.; Verbiest, T.; Persoons, A. *Macromol. Rapid Commun.* **2000**, *21*, 1. Yesodha, S. K.; Pillai, C. K. S.; Tsutsumi, N. *Prog. Polym. Sci.* **2004**, *29*, 45.

(5) Kajzar, F.; Lee, K. S.; Jen, A. K.-Y. *Adv. Polym. Sci.* **2003**, *161*, 1.

(6) Schottner, G. *Chem. Mater.* **2001**, *13*, 3422. Sanchez, C.; Lebeau, B.; Chaput, F.; Boilot, J. P. *Adv. Mater.* **2003**, *15*, 1969.

(7) Lebeau, B.; Brasselet, S.; Zyss, J.; Sanchez, C. *Chem. Mater.* **1997**, *9*, 1012.

(8) Lee, K. S.; Kim, T. D.; Min, Y. H.; Yoon, C. S. *Synth. Met.* **2001**, *117*, 311.

(9) Zhang, C.; Ren, A. S.; Wang, F.; Zhu, J. S.; Dalton, L. R. *Chem. Mater.* **1999**, *11*, 1966.

(10) Liu, S.; Haller, M. A.; Ma, H.; Dalton, L. R.; Jang, S.-H.; Jen, A. K.-Y. *Adv. Mater.* **2003**, *15*, 603.

(11) Zhang, H. X.; Lu, D.; Peyghambarian, N.; Fallahi, M.; Luo, J. D.; Chen, B. Q.; Jen, A. K.-Y. *Opt. Lett.* **2005**, *30*, 117.

(12) Jeng, R. J.; Chen, Y. M.; Jain, A. K.; Kumar, J.; Tripathy, S. K. *Chem. Mater.* **1992**, *4*, 972.

(13) Moylan, C. R.; Twieg, R. J.; Lee, V. Y.; Swanson, S. A.; Betterton, K. M.; Miller, R. D. *J. Am. Chem. Soc.* **1993**, *115*, 12599.

(14) Jeng, R. J.; Hung, W. Y.; Chen, C. P.; Hsiue, G. H. *Polym. Adv. Technol.* **2003**, *14*, 66.

(15) Behl, M.; Hattemer, E.; Brehmer, M.; Zentel, R. *Macromol. Chem. Phys.* **2002**, *203*, 503.

(16) Hua, J. L.; Li, B.; Meng, F. S.; Ding, F.; Qian, S. X.; Tian, H. *Polymer* **2004**, *45*, 7143.

(17) Lee, H. J.; Sohn, J.; Hwang, J.; Park, S. Y. *Chem. Mater.* **2004**, *16*, 456.

(18) Herman, W. N.; Hayden, L. M. *J. Opt. Soc. Am. B* **1995**, *12*, 416.

(19) Maker, P. D.; Terhune, R. W.; Nisenhoff, M.; Savage, C. M. *Phys. Rev. Lett.* **1962**, *8*, 21.

(20) Chen, L.; Qian, G.; Cui, Y.; Jin, X.; Wang, Z.; Wang, M. *J. Phys. Chem. B* **2006**, *110*, 19176.

(21) Broeck, K. V.; Verbiest, T.; Degryse, J.; Beylen, M. V.; Persoons, A.; Samyn, C. *Polymer* **2001**, *42*, 3315.

(22) Reyes-Esqueda, J.; Darracq, B.; Garcia-Macedo, J.; Canva, M.; Blanchard-Desce, M.; Chaput, F.; Lahlil, K.; Boilot, J. P.; Brun, A.; Levy, Y. *Opt. Commun.* **2001**, *198*, 207.

(23) Marder, S. R.; Beratan, D. N.; Cheng, L. T. *Science* **1991**, *252*, 103.

(24) Naoto, T.; Mikio, M.; Wataru, S. *Macromolecules* **1998**, *31*, 7764.

(25) Song, H. C.; Chen, Y. W.; Zheng, X. L.; Ying, B. N. *Spectrochim. Acta, Part A* **2001**, *57*, 1717.

(26) Palay, M. S.; Harris, J. M.; Looser, H.; Baumert, J. C.; Bjorklund, G. C.; Jundt, D.; Twieg, R. J. *J. Org. Chem.* **1989**, *54*, 3774.

(27) Hou, Z.; Liu, L.; Xu, L.; Chen, J.; Xu, Z.; Wang, W.; Li, F.; Ye, M. *Thin Solid Films* **1999**, *354*, 232.

(28) Sung, P. H.; Hsu, T. F.; Ding, Y. H.; Wu, A. Y. *Chem. Mater.* **1998**, *10*, 1642.

(29) Suzuki, A.; Matsuoka, Y. *J. Appl. Phys.* **1995**, *77*, 965.

(30) Corriu, R. J. P.; Moreau, J. J. E.; Thepot, P.; Man, M. W. C. *Chem. Mater.* **1992**, *4*, 1217.

(31) Pond, S. J. K.; Rumi, M.; Levin, M. D.; Parker, T. C.; Beljonne, D.; Day, M. W.; Brédas, J. L.; Marder, S. R.; Perry, J. W. *J. Phys. Chem. A* **2002**, *106*, 11470.

(32) Hohloch, M.; Maichle-Mošsmer, C.; Hanack, M. *Chem. Mater.* **1998**, *10*, 1327.

(33) Bartholomew, G. P.; Bazan, G. C.; Bu, X.; Lachicotte, R. J. *Chem. Mater.* **2000**, *12*, 1422.

(34) An, B. K.; Kwon, S. K.; Jung, S. D.; Park, S. Y. *J. Am. Chem. Soc.* **2002**, *124*, 14410.